This paper appears in IEEE Transactions on Haptics, 2012.
http://dx.doi.org/10.1109/TOH.2012.73

A Passivity Criterion for Sampled-data Bilateral Teleoperation Systems

Ali Jazayeri and Mahdi Tavakoli

Abstract

A teleoperation system consists of a teleoperator, a human operator, and a remote environment. Conditions involving system and controller parameters that ensure the teleoperator passivity can serve as control design guidelines to attain maximum teleoperation transparency while maintaining system stability. In this paper, sufficient conditions for teleoperator passivity are derived for when position error based controllers are implemented in discrete-time. This new analysis is necessary because discretization causes energy leaks and does not necessarily preserve the passivity of the system. The proposed criterion for sampled-data teleoperator passivity imposes lower bounds on the teleoperator's robots dampings, an upper bound on the sampling time, and bounds on the control gains. The criterion is verified through simulations and experiments.

Index Terms

Bilateral teleoperation, sampled-data passivity, discrete-time control

I. Introduction

A teleoperation system comprises of a human operator interacting with a master robot, and remotely controlling a slave robot, which is expected to perform a desired task on a remote environment. In designing controllers for such a system, stability is a prime issue that is investigated by many researchers. Stability of teleoperation systems is mainly jeopardized by two factors: (a) time delay in the communication channel, and (b) controller discretization. While the stability of delayed teleoperation systems has been widely studied in the literature [1], [2], we contemplate the impact of the discrete-time controllers on the passivity of the teleoperator, which includes a master robot, a slave robot, their controllers, and a communication channel. The communication channel is assumed to be delay-free, which requires the master and the slave robot to be physically close to each other. An example of this situation is robotics-assisted surgical systems where the master and the slave robots are in the same room.

Due to the unknown, time-varying and sometimes nonlinear dynamics of the environment and/or the operator, it is easier to analyze the passivity of the teleoperator in lieu of the stability of the closed-loop teleoperation system (Fig. 1). Indeed, the interconnection of a passive teleoperator with passive environment and operator terminations will be passive and consequently stable [3]. For a bilateral teleoperation system in continuous-time, the teleoperator is modelled as a 2-port network and subsequently the teleoperator passivity condition is related to the scattering matrix of the 2-port network [1]. Alternatively, the passivity of the continuous-time teleoperator can be analyzed by Raisbeck's condition [4], [5].

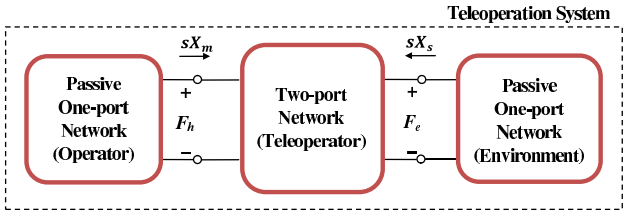

Fig. 1. The passivity of the teleoperation system is guaranteed when the 2-port network teleoperator is passive and connected to two passive 1-port network terminations.

The passivity of a teleoperation system is not guaranteed once the continuous-time controllers are substituted with their discrete-time counterparts because of energy leaks caused by the zero order hold (ZOH) [6]. A zero-order hold accounts for half-sample delay (not to be confused with the communication channel's delay) and has energy-instilling effects.

Similar to bilateral teleoperation, in a force-reflective virtual reality simulation system, the operator feels virtual contact forces while applying position commands through the haptic user interface. Colgate and Schenkel found a passivity condition for such a system considering the discrete-time components of the system [7]. The passivity condition for the discrete simulation of a virtual wall $K + sB$ was found to be $b > KT/2 + B$, where b is the haptic interface damping and T is the sampling time. The stability of the virtual wall system has also been investigated using the Routh-Hurwitz method [8]; the condition for the stability of the same system is $b > KT/2 - B$, which is clearly less conservative than the passivity condition. Previous research has also considered the impact of other non-idealities such as quantization and friction on the stability of the virtual wall system [9], [10]. While the effects of energy leaks caused by discretization have been thoroughly investigated for haptic interaction with a virtual wall [8], [9], we consider the effect of discretization components for the case of haptic interaction

This research was supported by the Natural Sciences and Engineering Research Council (NSERC) of Canada under grants RGPIN-372042 and EQPEQ 375712. Authors are with the Department of Electrical and Computer Engineering at the University of Alberta, Canada.
Emails: {ali.jazayeri, mahdi.tavakoli}@ualberta.ca.

with a physical environment via a computer-controlled teleoperation system. In this paper, we will find passivity conditions that can be used in control design to achieve maximum transparency and enable the human to stably teleoperate in the presence of discretization components.

In some approaches to studying sampled-data teleoperation, the entire teleoperation system is converted to either the discrete-time domain [11] or the continuous-time domain [12], which simplifies the stability analysis for known models of the environment and the operator. Also, Hannaford et al. proposed a passivity observer / passivity controller for monitoring and controlling the energy in the communication channel of a discrete-time teleoperation system [13]. In addition, Stramigioli et al. proposed a geometric method to investigate the problem of having both continuous-time and discrete-time signals in a single system where the teleoperation system is represented by a continuous-time port-Hamiltonian system [14], [15].

In this paper, the passivity analysis starts with considering the dynamics of the master and the slave controllers as well as the dynamics of the master and the slave robots. Then, we will derive a passivity condition for a sampled-data teleoperation system with a position-error-based controller architecture. The passivity conditions will impose bounds on the system parameters such as the sampling time, the controller gains, and the robots damping. It is important to determine the lower bound on the damping term of the robots as most of the newly designed haptic devices intentionally have low damping terms to deliver touch sensitivity and fidelity to the operator. The upper bounds on the controllers gains give a useful guideline for control design as the transparency of the teleoperation system is degraded if the control gains are small in the stable region [16]. Thus, the results of this paper can be viewed as conditions that can be used as design guidelines for achieving highly transparent yet stable teleoperation.

The rest of this paper is organized as follows. The teleoperation system is modelled in Section II and this model is used in Section III to find a condition for the passivity of the teleoperator. This condition has been tested via computer simulations in Section IV, which allows the flexibility to charge the damping terms of the robots (they are fixed in the experiments). Then, the experimental results using two Phantom Premium robots are reported in Section V, and concluding remarks are given in Section VI.

II. Teleoperation System Modelling

A diagram of a position-error-based sampled-data teleoperation system is shown in Fig. 2. The master and the slave robots are modelled as 1-degree-of-freedom (1-DOF), linear time invariant (LTI) systems

$$\begin{aligned} f_h - f_m &= m_m \ddot{x}_m + b_m \dot{x}_m \\ f_e - f_s &= m_s \ddot{x}_s + b_s \dot{x}_s \end{aligned} \tag{1}$$

The subscripts m and s indicate the master and the slave robots, respectively. In (1), f_i's are the controller output forces and x_i's are the robots positions and f_h and f_e are the human operator and the environment forces. Also, m and b denote the mass and the damping of each robot. It is also assumed that the robots do not include link or joint flexibility. The environment and the operator are modelled as LTI impedances $Z_e(s)$ and $Z_h(s)$, which are assumed to be passive but otherwise arbitrary. In Fig. 2, $\tilde{f}_h$ is the exogenous input force from the operator's hand and $\tilde{f}_e$ is the exogenous input force from the environment.

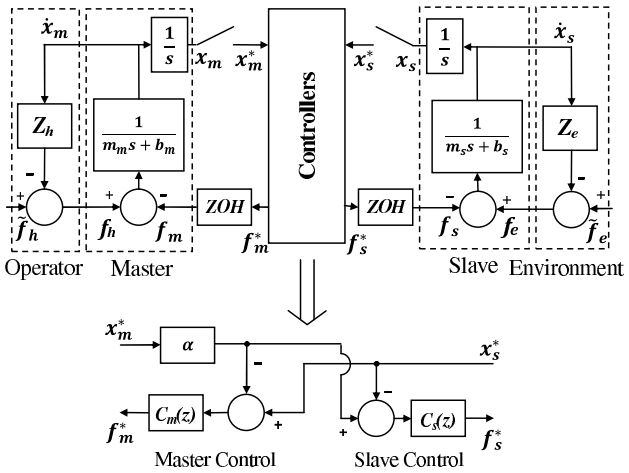

Fig. 2. The block diagrams of a teleoperation system, which includes discretized controller models.

As depicted in Fig. 2, the positions of the master and slave robots are discretized using samplers blocks. The superscript * denotes sampled signals. The sampled signals are converted back to the continuous-time domain using zero-order-hold blocks. The environment and the operator LTI models of Fig. 2 can be written in the Laplace domain as

$$\begin{aligned} \tilde{F}_h(s) - F_h(s) &= Z_h(s) s X_m(s) \\ \tilde{F}_e(s) - F_e(s) &= Z_e(s) s X_s(s) \end{aligned} \tag{2}$$

The robots' dynamics (1) can be rewritten in the Laplace domain as

$$\begin{aligned} sX_m(s) &= \frac{1}{m_m s + b_m}(F_h(s) - F_m(s)) \\ sX_s(s) &= \frac{1}{m_s s + b_s}(F_e(s) - F_s(s)) \end{aligned} \tag{3}$$

The output of the sampler can be mathematically represented as a Dirac comb weighted by the sampled signal [17], i.e., $x^*(t) = \sum_{k=0}^{\infty} x(kT)\delta(t - kT)$ and the mathematical representation of the sampled signal in the Laplace domain is

$$X^*(s) = \mathcal{L}\{x^*(t)\} = \sum_{k=0}^{\infty} x(kT)e^{-skT} \tag{4}$$

The z-domain equivalent of (4) is $X(z) = \mathcal{Z}\{x^*(t)\} = X^*(s)|_{s=1/T \ln z}$. The ZOH block's transfer function relating its discrete-time input to its continuous-time output is [18]

$$F_m(s) = \frac{1 - e^{-sT}}{sT} F_m^*(s), F_s(s) = \frac{1 - e^{-sT}}{sT} F_s^*(s) \tag{5}$$

The position error based (PEB) controller blocks in Fig. 2 apply forces based on the master/slave position difference. The position error is defined as

$$e = x_m - x_s \tag{6}$$

The discrete-time controllers of the master and the slave implement the following control laws

$$\begin{aligned} F_m^*(s) &= C_m(z)|_{z=e^{sT}}[X_s^*(s) - X_m^*(s)] \\ F_s^*(s) &= C_s(z)|_{z=e^{sT}}[X_m^*(s) - X_s^*(s)] \end{aligned} \tag{7}$$

III. Passivity condition for the sampled-data teleoperator

The teleoperator passivity condition in the time domain is based on the dissipated energy in the equivalent 2-port network of the teleoperator, which can be measured by the input-output energy integral at the two ports (Fig. 1). For the 2-port network initially at rest, the passivity condition is

$$\int_0^t f_h(\tau)\dot{x}_m(\tau)d\tau + \int_0^t f_e(\tau)\dot{x}_s(\tau)d\tau > 0 \tag{8}$$

The teleoperator is passive if and only if, for all time $t > 0$, (8) holds. Condition (8) will be satisfied if

$$\int_0^t f_h(\tau)\dot{x}_m(\tau)d\tau + \int_0^t f_e(\tau)\dot{x}_s(\tau)d\tau > \frac{1}{2}m_m\dot{x}_m^2 + \frac{1}{2}m_s\dot{x}_s^2 \tag{9}$$

Clearly, (9) is sufficient but not necessary for (8). The dynamics of the master robot in (1) implies that

$$f_h - f_m = m_m\frac{d\dot{x}_m}{dt} + b_m\dot{x}_m \tag{10}$$

Finding f_h from (10) and substituting it in (9), along with similar simplifications for the slave robot, simplifies (9) to

$$\begin{aligned} &\int_0^t f_m(\tau)\dot{x}_m(\tau)d\tau + \int_0^t f_s(\tau)\dot{x}_s(\tau)d\tau \\ &+ \int_0^t b_m\dot{x}_m^2(\tau)d\tau + \int_0^t b_s\dot{x}_s^2(\tau)d\tau > 0 \end{aligned} \tag{11}$$

A generalization of the Parseval's theorem [19] can be used to take (11) to the frequency domain as

$$\begin{aligned} &\int_{-\infty}^{\infty} F_m(j\omega)V_m^c(j\omega)d\omega + \int_{-\infty}^{\infty} F_s(j\omega)V_s^c(j\omega)d\omega + \\ &\int_{-\infty}^{\infty} b_m V_m(j\omega)V_m^c(j\omega)d\omega + \int_{-\infty}^{\infty} b_s V_s(j\omega)V_s^c(j\omega)d\omega > 0 \end{aligned} \tag{12}$$

where V_i and F_i (for $i = m, s$) are the Fourier transforms of $\dot{x}_i$ and f_i, respectively, and the superscript ^{c} denotes the complex conjugate operator.

Based on (5) and (7), the control signals for the master and the slave are

$$\begin{aligned} F_m(j\omega) &= -\frac{1}{j\omega}\bar{C}_m(j\omega)X_m^*(j\omega) + \frac{1}{j\omega}\bar{C}_m(j\omega)X_s^*(j\omega) \\ F_s(j\omega) &= -\frac{1}{j\omega}\bar{C}_s(j\omega)X_m^*(j\omega) + \frac{1}{j\omega}\bar{C}_s(j\omega)X_s^*(j\omega) \end{aligned} \tag{13}$$

where

$$\bar{C}_m(j\omega) = -\frac{1-e^{-j\omega T}}{T} C_m(e^{j\omega T})$$
$$\bar{C}_s(j\omega) = -\frac{1-e^{-j\omega T}}{T} C_s(e^{j\omega T}) \tag{14}$$

The sampled positions in (13) can be found from (4) as

$$X_m^*(j\omega) = \frac{1}{T}\sum_{n=-\infty}^{\infty} \frac{V_m(j\omega + jn\omega_s)}{j\omega + jn\omega_s}$$
$$X_s^*(j\omega) = \frac{1}{T}\sum_{n=-\infty}^{\infty} \frac{V_s(j\omega + jn\omega_s)}{j\omega + jn\omega_s} \tag{15}$$

where $\omega_s = 2\pi/T$. Substituting (13) and (15) into the first two terms of (12) simplifies the latter to

$$\begin{aligned}
&\int_{-\infty}^{\infty} \bar{C}_m(\omega) \sum_{n=-\infty}^{\infty} \frac{V_m(j\omega + jn\omega_s) - V_s(j\omega + jn\omega_s)}{j\omega + jn\omega_s} \\
&\times \left[\frac{V_m(j\omega)}{j\omega}\right]^c d\omega \\
+&\int_{-\infty}^{\infty} \bar{C}_s(\omega) \sum_{n=-\infty}^{\infty} \frac{V_s(j\omega + jn\omega_s) - V_m(j\omega + jn\omega_s)}{j\omega + jn\omega_s} \\
&\times \left[\frac{V_s(j\omega)}{j\omega}\right]^c d\omega
\end{aligned} \tag{16}$$

To further simplify (16), the master and the slave controllers are selected to be equal to each other:

$$C_m(j\omega) = C_s(j\omega) = C(j\omega) \tag{17}$$

In a special case later in this section, the assumption (17) will be altered to cover a more general case where the controllers are proportional to each other with the same scaling factor as the position scaling factor.

For simplicity of notation, let us define $\bar{C}(j\omega) = \bar{C}_m(j\omega)$. Then, (16) can be rewritten as

$$\int_{-\infty}^{\infty} \bar{C}(j\omega) \sum_{n=-\infty}^{\infty} \frac{V(j\omega + jn\omega)}{j\omega + jn\omega} \left[\frac{V(j\omega)}{j\omega}\right]^c d\omega \tag{18}$$

where $V(j\omega)$ is defined as

$$V(j\omega) = V_m(j\omega) - V_s(j\omega) \tag{19}$$

Using Lemma 1 in Appendix , $\bar{C}(j\omega)$ can be replaced by its real value

$$\int_{-\infty}^{\infty} \mathrm{Re}\{\bar{C}(\omega)\} \sum_{n=-\infty}^{\infty} \frac{V(j\omega + jn\omega)}{j\omega + jn\omega} \left[\frac{V(j\omega)}{j\omega}\right]^c d\omega \tag{20}$$

Now, (20) can be split to two parts based on the sign of the real part of the transfer function $\bar{C}$ as

$$\begin{aligned}
&\int_{-\infty}^{\infty} \bar{C}^+(j\omega) \sum_{n=-\infty}^{\infty} \frac{V(j\omega + jn\omega)}{j\omega + jn\omega} \left[\frac{V(j\omega)}{j\omega}\right]^c d\omega \\
+&\int_{-\infty}^{\infty} \bar{C}^-(j\omega) \sum_{n=-\infty}^{\infty} \frac{V(j\omega + jn\omega)}{j\omega + jn\omega} \left[\frac{V(j\omega)}{j\omega}\right]^c d\omega
\end{aligned} \tag{21}$$

where

$$\bar{C}^+(j\omega) = \begin{cases} \mathrm{Re}\{\bar{C}(j\omega)\} & , \text{if } \mathrm{Re}\{\bar{C}(j\omega)\} > 0 \\ 0 & , \text{otherwise} \end{cases} \tag{22}$$

$$\bar{C}^-(j\omega) = \begin{cases} \mathrm{Re}\{\bar{C}(j\omega)\} & , \text{if } \mathrm{Re}\{\bar{C}(j\omega)\} < 0 \\ 0 & , \text{otherwise} \end{cases} \tag{23}$$

Lemma 2 in Appendix shows that the first integral in (21) is positive at all time.

Therefore, using (16) and (21), a sufficient condition (12) for the teleoperator passivity becomes

$$\int_{-\infty}^{\infty} \bar{C}^{-}(\omega) \sum_{n=-\infty}^{\infty} \frac{V(j\omega + jn\omega)}{j\omega + jn\omega} \left[\frac{V(j\omega)}{j\omega}\right]^{c} d\omega + \int_{-\infty}^{\infty} b_m V_m(j\omega) V_m^c(j\omega) d\omega + \int_{-\infty}^{\infty} b_s V_s(j\omega) V_s^c(j\omega) d\omega > 0 \tag{24}$$

Using Lemma 3 in Appendix , the first integral in (24) is greater than

$$\int_{-\infty}^{\infty} \bar{C}^{-}(\omega) \sum_{n=-\infty}^{\infty} \frac{1}{(\omega + n\omega_s)^2} V(j\omega) V^c(j\omega) d\omega \tag{25}$$

Thus, for passivity of the teleoperator it is sufficient to have

$$\int_{-\infty}^{\infty} \bar{C}^{-}(\omega) \sum_{n=-\infty}^{\infty} \frac{1}{(\omega + n\omega_s)^2} V(j\omega) V^c(j\omega) d\omega + \int_{-\infty}^{\infty} b_m V_m(j\omega) V_m^c(j\omega) d\omega + \int_{-\infty}^{\infty} b_s V_s(j\omega) V_s^c(j\omega) d\omega > 0 \tag{26}$$

The definition of $V(j\omega)$ can be substituted from (19) in (26). Then, the first integral in (26) becomes

$$\begin{aligned} &\int_{-\infty}^{\infty} \bar{C}^{-}(\omega) \sum_{n=-\infty}^{\infty} \frac{1}{(\omega + n\omega_s)^2} V_m(j\omega) V_m^c(j\omega) d\omega \\ &+ \int_{-\infty}^{\infty} \bar{C}^{-}(\omega) \sum_{n=-\infty}^{\infty} \frac{1}{(\omega + n\omega_s)^2} V_s(j\omega) V_s^c(j\omega) d\omega \\ &- \int_{-\infty}^{\infty} \bar{C}^{-}(\omega) \sum_{n=-\infty}^{\infty} \frac{1}{(\omega + n\omega_s)^2} \\ &\times \left\{V_m(j\omega) V_s^c(j\omega) + V_m^c(j\omega) V_s(j\omega)\right\} d\omega \end{aligned} \tag{27}$$

Applying Lemma 4 in Appendix to the last integral in (27), it can be said that (27) is less than

$$\begin{aligned} &\int_{-\infty}^{\infty} \bar{C}^{-}(\omega) \sum_{n=-\infty}^{\infty} \frac{1}{(\omega + n\omega_s)^2} V_m(j\omega) V_m^c(j\omega) d\omega + \\ &\int_{-\infty}^{\infty} \bar{C}^{-}(\omega) \sum_{n=-\infty}^{\infty} \frac{1}{(\omega + n\omega_s)^2} V_s(j\omega) V_s^c(j\omega) d\omega \\ &+ \int_{-\infty}^{\infty} \bar{C}^{-}(\omega) \sum_{n=-\infty}^{\infty} \frac{1}{(\omega + n\omega_s)^2} \\ &\times \left\{V_m(j\omega) V_m^c(j\omega) + V_s^c(j\omega) V_s(j\omega)\right\} d\omega \end{aligned} \tag{28}$$

Ultimately, Lemma 5 in Appendix shows that (28) and the last two integrals of (26) result in a sufficient condition for passivity of the teleoperator as

$$\boxed{\begin{aligned} b_m &> \frac{T}{1 - \cos\omega T} \operatorname{Re}\left\{(1 - e^{-j\omega T}) C_m(e^{j\omega T})\right\} \\ b_s &> \frac{T}{1 - \cos\omega T} \operatorname{Re}\left\{(1 - e^{-j\omega T}) C_s(e^{j\omega T})\right\} \end{aligned}} \tag{29}$$

A. A more general case: Unequal controllers

The restriction that the master and slave controllers be identical may be relaxed:

$$\frac{C_m(j\omega)}{\alpha} = C_s(j\omega) = C(j\omega) \tag{30}$$

where α is a position scaling factor for the master and the slave, respectively. It should be noted that setting the controllers to the same proportion as the position signals is practically justifiable. For instance, in micro-surgery, the slave's micro-surgical tools undergo fine motions and need a higher-gain controller compared to the master's handle whose range of motion spans the human hand's workspace (i.e., $C_m < C_s$ and $x_m > x_s$). The assumption (30), which serves as a requisite for the passivity of the teleoperator, has also been made in similar passivity analyses for continuous-time bilateral teleoperation systems [20], [21]. In the case of (30), the position error (6) becomes

$$e = \alpha x_m - x_s \tag{31}$$

We repeated the previous analysis for the case of (30) and (31), but do not show the steps for brevity. The resulting passivity condition in the unequal controller case is

$$\boxed{\begin{aligned} b_m &> \frac{T}{2}\frac{\alpha+1}{1-\cos\omega T}\,\mathrm{Re}\left\{(1-e^{-j\omega T})C_m(e^{j\omega T})\right\} \\ b_s &> \frac{T}{2}\frac{\alpha+1}{1-\cos\omega T}\,\mathrm{Re}\left\{(1-e^{-j\omega T})C_s(e^{j\omega T})\right\} \end{aligned}} \tag{32}$$

B. A special case: PD controller

The passivity condition (29) is valid for all controllers $C_m = C_s$. If the controller's structure is known, the condition can be further simplified. For instance, for a PD controller $K + Bs$, which can be discretized using bilinear transformation method as

$$C_s(z) = C_m(z) = K + B\frac{z-1}{Tz} \tag{33}$$

the passivity condition (29) simplifies to

$$b > KT - 2B\cos\omega T \tag{34}$$

where b is the minimum of b_s and b_m. Condition (34) is dependent on the frequency ω. The term $\cos\omega T$ can vary between -1 and 1. Thus, a sufficient condition for teleoperator passivity over all frequencies will be

$$b > KT + 2B \tag{35}$$

which has to hold for both the master and the slave robots.

Condition (35) implies that increasing the sampling time and controller gains drive the teleoperator closer to non-passivity. The robot damping b is a physical characteristic of the robot and cannot be easily changed whereas the other parameters in (35) can be appropriately set in the control design process. In addition to the passivity of the teleoperator, it is desirable to have high teleoperation transparency. In a continuous-time teleoperation system, increasing the controller gains makes the system more transparent. Condition (35) can be used to achieve as high a transparency as possible while maintaining passivity in a sampled-data teleoperation system. It is interesting to note that the passivity condition (35) for the teleoperation system with equal PD controllers (33) for the master and the slave has coincided with the passivity condition for a system involving haptic interaction with a discretely-simulated virtual wall as investigated by Colgate and Schenkel [7].

IV. Simulation study

The teleoperation system of Fig. 2 has been simulated in MATLAB/Simulink and the passivity condition (35) has been tested for a teleoperator comprising a pair of 1-DOF robots modelled by mass and damping terms. These mass and damping parameters match those of Phantom Premium 1.5A robots used in the experiments, the details of which will be described in Section V. The simulation allows for variation of parameters that cannot be altered in experiments such as the robot damping term b.

To determine the passivity of the teleoperator, a passivity observer, which calculates the dissipated energy, has been incorporated into the simulations. The dissipated energy is represented by the input-output energy integral in (8). For a passive teleoperator, the energy integral is non-negative at all times.

For selected model parameters, first the passivity borderline is theoretically determined via condition (35) and shown in Fig. 3 by red lines. Next, the simulation is repeated for various model parameters changed over a grid in the parameter space. The system is simulated for a chosen passive model (a first-order positive-real transfer function) for the human operator and the environment. Changing the model of the human operator and the environment – zero impedance, infinite impedance, or other positive-real transfer functions yields similar simulation results, which have been omitted for brevity. In each point of the grid of parameters values, the energy integral is monitored to detect non-passive teleoperator cases; if the energy integral becomes negative at any time, it signals a non-passive teleoperator. The dark pixels in Fig. 3 indicate where in the parameter space the energy integral becomes negative (i.e., the teleoperator is non-passive). As it can be seen, the regions indicated by the passivity condition (35) closely match the simulation results. There is a gap between the filled area and the red line, which corresponds to cases where condition (35) is conservative for detecting the teleoperator non-passivity. The conservatism of condition (35) was predictable due to the fact that it was found as a sufficient condition for passivity.

V. Experimental results

A. Teleoperation system setup

To verify the passivity condition (35) experimentally, the stability condition has been tested for a teleoperation system consisting of a pair of Phantom Premiums 1.5A robots (Sensable Technologies/Geomagic, Wilmington, MA) with JR3 force sensors (JR3, Inc., Woodland, CA) at their end-effectors. We consider the robots to work in the joint space – angular position and torque are the output and input of each joint of each robot. Out of the three actuated joints of each robot, the first one is used in the experiment while the second and the third joints, which form a parallel mechanism, are locked using high gain controllers.

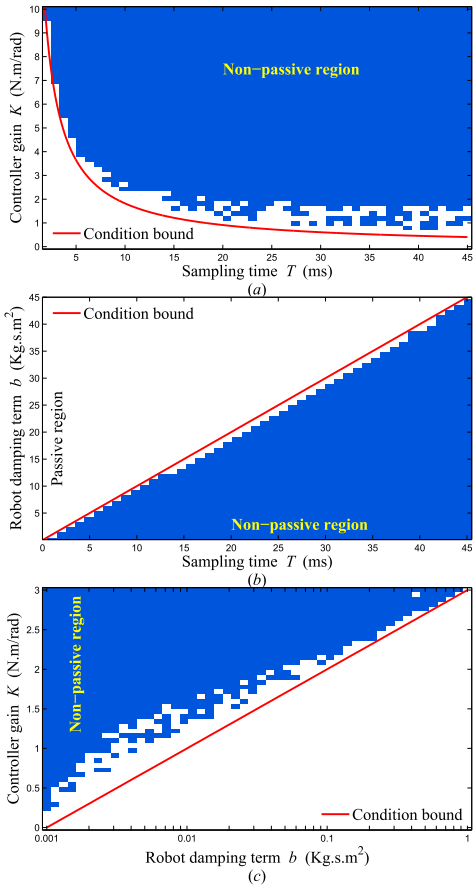

Fig. 3. Passive and non-passive regions (a) in $K-T$ plane for $B=0$ $m=0.015$ and $b=0.01822$, (b) in $b-T$ plane for $K=1$, $m=0.015$ and $B=0$, and (c) in $K-b$ plane for $B=0$, $m=0.015$ and $T=1^{\text{ms}}$.

B. Choice of terminations: Free-motion/free-motion (FF) vs. free-motion/clamped (FC)

The experiments have set up to include two extreme cases of zero and infinitely-stiff impedances corresponding to free-motion and a clamped coupling for each termination. This results in four combinations for the two terminations.

- Case 1: Both master and slave in free motion (FF)
- Case 2: Master in free motion and slave clamped (FC)
- Case 3: Master clamped and slave in free motion (FC)
- Case 4: Both master and slave clamped (CC)

Since our teleoperation system including its controllers is symmetric with respect to the master and the slave, Cases 2 and 3 are similar experiments (FC). In contrast to Cases 1 to 3 for the termination choices where at least one of the robots is able to move and potentially show the instability of the teleoperation system, Case 4 does not serve our experiment objectives. Having clamped robots allows for non-zero forces, but does not allow for the investigation of stability in our position-error-based teleoperation system. Thus, Case 4 has been excluded from our experiments. Case 4 (CC) can be important as one of the extreme cases for termination choices especially in control architectures with force sensor feedback (e.g., the 4-channel method) where the destabilizing effect of non-collocated sensing and link/joint flexibility are important. Fig. 4 shows the experimental setup for the FC termination arrangement, and the FF arrangement (not shown) is similar except that it involves no clamping of either robot.

It should be noted that the experimental protocol described above has the advantage that it is independent of any human operator's intervention (as master's coupling), rendering the experiments highly reproducible. Similarly, it does not depend on any particular physical environment (as slave's coupling).

Within each of the two *cases* for the terminations (FF or FC), different *experiments* have been run for different values of the sampling time. Within each experiment (i.e., at a given sampling time), the controller gain has been altered in different *tests*. Within each test (i.e., at a given sampling time and a given controller gain), different *trials* have been conducted for different values of the initial condition.

C. Choice of initial conditions

In the experiments, when the master and/or the slave are in free motion, we provide them with initial conditions such that the teleoperation system is excited; otherwise, there will be no motion. The initial condition specifies the position difference

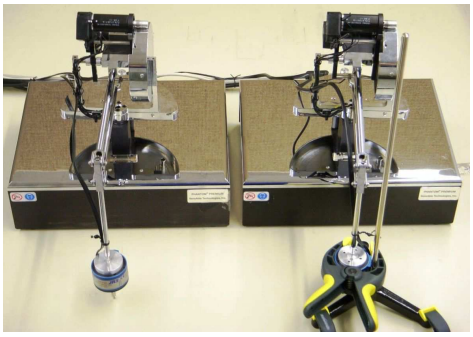

Fig. 4. Experimental setup for the case where the master arm (left) is in free motion and the slave arm (right) is clamped (FC).

between the master and the slave at the onset of a trial (within a test within an experiment) – the slave is placed at the origin of its coordinate system while the master has an initial angular position. Since a passive system should remain stable regardless of its initial condition, when investigating the passivity of the teleoperator, the initial condition has been changed over a series of trials in a large span only limited by the physical constraints of the experimental setup. Instability in one trial is enough to indicate that the teleoperation system with the chosen parameters is potentially unstable. If none of the trials makes the teleoperation system unstable, the system is identified as passive at this particular test (with controller gain K) and experiment (with sampling time T).

D. Determination of passivity/non-passivity borderline

In both FF and FC cases, either the velocity or the contact force is zero in both the master and the slave sides. This makes the passivity definition according to the integral of power at the two ports, namely (8), impossible to check because the power at each port is always zero. Instead, to determine the non-passivity of the teleoperation system, its instability has been monitored as characterized by growing oscillations. It should be noted that the reverse conclusion is not valid; there are systems that are stable without being passive.

The procedure for experimentally determining the passivity/non-passivity borderline is as follows. A given sampling time T specifies a vertical line in the $K-T$ plane for different values of the controller gain K. The intersection of this vertical line with the theoretical passivity borderline determines the value of the controller gain below (above) which the teleoperator is expected – from a purely theoretical perspective – to be passive (non-passive). The objective of each experiment is to find the smallest and the largest controller gains that make the teleoperator non-passive and passive, respectively, at a given sampling time. Such an experiment is then repeated at different sampling times (vertical line locations). To find the smallest controller gain that makes the teleoperator non-passive, the controller gain is first set to the value given by the theoretical passivity borderline at that sampling time. Next, we perform a trial for a small initial condition, the results of which can be one of the following two possibilities.

- (A) If the teleoperation system is stable, the trial is repeated with a larger initial condition. The increase in the initial condition is continued until either the system becomes unstable (reverting to Case B below) or the entire range of initial conditions has been tested. If no instability was observed across the trials, the data point corresponding to this test is marked as being passive in the $K-T$ plane. Then, the controller gain is increased slightly (by steps of less than 1% of the maximum gain) and the same test is repeated for this new gain, possibly adding one more passive data point to the $K-T$ plane. The increase in the controller gain is continued until the system becomes unstable, which corresponds to a non-passive teleoperation system.
- (B) If the teleoperation system is unstable, the data point corresponding to this test is marked as being non-passive in the $K-T$ plane. Then, following a procedure in the opposite direction, the controller gain is decreased slightly (by steps of less than 1% of the maximum gain) until the system becomes stable. Again, if no instability was observed across several trials, the data point corresponding to this test is marked as being passive in the $K-T$ plane.

The result of the above procedure is an accurate experimentally-obtained passivity borderline in the $K-T$ plane.

E. Results

The experimental borderlines found for FF and FC experiments are shown in Fig. 5 and 6, respectively. Thus, in Fig. 5, the teleoperator is coupled to two zero-impedance terminations. Also, in Fig. 6, the teleoperator is coupled to a zero-impedance termination and another infinite-impedance termination. The theoretical regions of passivity and (potential) non-passivity obtained from condition (35) are shown as separated by the theoretical borderline (blue line). Also, the result of each experiment is indicated either as a star (stable) or a circle (unstable) in these figures. For a given sampling time, many more tests were conducted but not shown in Fig. 5 and 6; only those data points corresponding to the previously-discussed "smallest and the largest controller gains" were shown.

As seen in Fig. 5, in the FF case, the theoretical teleoperator passivity/non-passivity borderline closely matches the experimentally-obtained borderline. The close match between the theoretical borderline (35) for the passivity of the teleoperator and the experimental borderline for the stability of the teleoperation system in the FF case (Fig. 5) demonstrates that the aforementioned

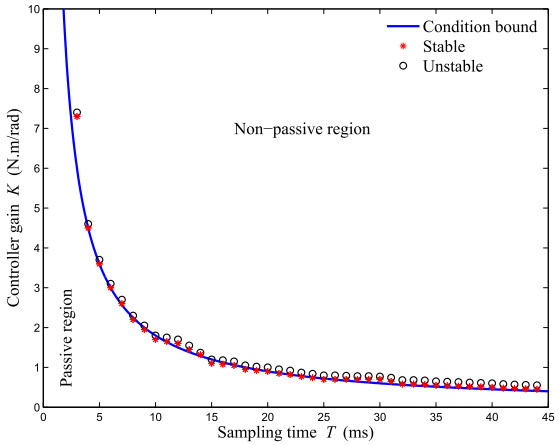

Fig. 5. Free-motion/free-motion (FF) experiment data points and theoretical passivity borderline. Stars represent stable, and circles represent unstable systems.

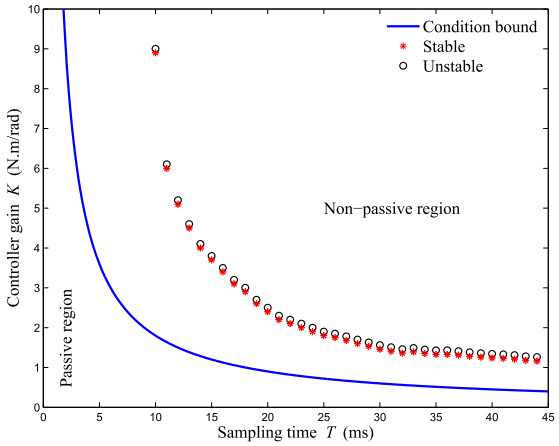

Fig. 6. Free-motion/clamped (FC) experiment data points and theoretical passivity borderline. Stars represent stable, and circles represent unstable systems.

theoretical condition is not overly conservative in the context of stability analysis. Also, this theoretical condition corresponds to a worst-case scenario in terms of termination choices the stability region for the teleoperation system in the FC case (Fig. 6) is bigger than that predicted by the passivity region for the teleoperator in the FF case (Fig. 5). From Fig. 6, in the FC case, it is seen that the theoretical teleoperator passivity/non-passivity borderline is more conservative than the experimentally-obtained borderline in the sense that, in the $K-T$ plane, certain theoretically non-passive points are found to be practically passive. Both of the above were expected for the reasons explained below. Recall that we defined a teleoperation system to consist of a teleoperator coupled to two terminations (a human operator and a remote environment). In the FF case, the teleoperation system and the teleoperator are the same and, therefore, the non-passivity of the teleoperation system (as assessed by the procedure outlined in Section V-D) is tantamount to the (potential) non-passivity of the teleoperator (as assessed by condition (35)). However, in the FC case, the experimental procedure to determine passivity/non-passivity in Section V-D concerns that of the teleoperation system, which is now different from the teleoperator alone due to the presence of one infinitely-stiff termination for the teleoperator. In other words, while the choice of terminations cannot affect the passivity or nonpassivity of the teleoperator, it affects the stability of the overall teleoperation system, which is what is evaluated through the steps in Section V-D. Thus, the theoretical passive region (35) for the teleoperator was expected to be different from the experimental non-passive region for the teleoperation system with the gap between these two regions being affected by the passive behaviors of the terminations. The extreme FF and FC cases for terminations in Fig. 4 correspond to two of the possible extreme passivity/non-passivity borderlines.

F. Transparency comparison

From the passivity borderlines in Fig. 5 and Fig. 6, it can be concluded that the upper bound on the controller gain becomes smaller as the sampling time increases. For any given sampling time, one may choose the controller gain to be low enough to avoid instability of the teleoperation system. However, lowering the controller gain comes at a cost to transparency of the teleoperation system; to limit the transparency degradation, we need to use the largest stabilizing controller gain. Table I demonstrates this fact using free-motion experiments in which the controller gain K and the sampling time T are altered and master-slave position tracking error is measured: in most cases increasing K in the stable region of the $K-T$ plane results

TABLE I
MEAN-SQUARE-ERROR OF MASTER-SLAVE POSITION TRACKING RELATIVE TO THE MASTER POSITION MEAN-SQUARE (PERCENT).

T (ms)	$K = 0.4$	$K = 1.0$	$K = 2.0$	$K = 2.4$
7	10.2580	9.9864	3.0355	3.3159
15	13.2608	5.8948	Unstable	Unstable

in smaller percent mean-square-error (MSE) in position tracking relative to the mean-square-error of master position. This is why knowing the passivity borderline is important.

VI. CONCLUSIONS

In this paper, a passivity condition has been found for a delay-free bilateral teleoperation system in which the position error based controllers are implemented in discrete-time. To find this condition, the models of the zero-order-hold and the sampler are incorporated in an appropriate frequency-domain analysis. The condition imposes a lower bound on the robot damping, an upper bound on the sampling time, and bounds on the controller gains. For the special case of PD control, the bounds on the proportional and derivative controller gains have been found to be upper bounds. Thus, the passivity condition provides the designer with guidelines about how much the controller gain can be increased with no risk of instability. Supporting simulations and experiments demonstrating the validity of the passivity condition have been reported.

REFERENCES

[1] R. J. Anderson and M. W. Spong, "Asymptotic Stability for Force Reflecting Teleoperators with Time Delay," *The International Journal of Robotics Research*, vol. 11, no. 2, pp. 135–149, 1992.
[2] G. Niemeyer and J.-J. Slotine, "Stable adaptive teleoperation," *Oceanic Engineering, IEEE Journal of*, vol. 16, no. 1, pp. 152 –162, 1991.
[3] P. F. Hokayem and M. W. Spong, "Bilateral teleoperation: An historical survey," *Automatica*, vol. 42, no. 12, pp. 2035–2057, 2006.
[4] S. Haykin, *Active Network Theory*. Reading, MA: Addison-Wesley, 1970.
[5] V. Mendez and M. Tavakoli, "A passivity criterion for n-port multilateral haptic systems," in *Proceedings of Conference on Decision and Control*, Atlanta, GA, 2010, pp. 3608–3613.
[6] M. Tavakoli, A. Aziminejad, R. Patel, and M. Moallem, "Discrete-time bilateral teleoperation: modelling and stability analysis," *Control Theory and Applications, IET*, vol. 2, no. 6, pp. 496–512, 2008.
[7] E. Colgate and G. Schenkel, "Passivity of a class of sampled-data systems: Application to haptic interfaces," *Journal of Robotic Systems*, vol. 14, no. 1, pp. 37–47, 1997.
[8] J. Gil, A. Avello, A. Rubio, and J. Florez, "Stability analysis of a 1 DOF haptic interface using the routh-hurwitz criterion," *IEEE Transactions on Control Systems Technology*, vol. 12, no. 4, pp. 583–588, 2004.
[9] N. Diolaiti, G. Niemeyer, F. Barbagli, and J. J.K. Salisbury, "Stability of haptic rendering: discretization, quantization, time delay, and coulomb effects," *IEEE Transactions on Robotics*, vol. 22, no. 2, pp. 256– 268, 2006.
[10] J. Abbott and A. Okamura, "Effects of position quantization and sampling rate on virtual wall passivity," *IEEE Transactions on Robotics*, vol. 21, no. 5, pp. 952–964, 2005.
[11] P. Berestesky, N. Chopra, and M. Spong, "Discrete time passivity in bilateral teleoperation over the Internet," in *Proceedings of International Conference on Robotics and Automation*, New Orleans, LA, 2004, pp. 4557–4564.
[12] K. Kosuge and H. Murayama, "Bilateral feedback control of telemanipulator via computer network in discrete time domain," in *Proceedings of IEEE International Conference on Robotics and Automation, 1997*, vol. 3, 1997, pp. 2219–2224.
[13] J. H. Ryu, D. S. Kwon, and B. Hannaford, "Stable teleoperation with time-domain passivity control," *IEEE Transactions on Robotics and Automation*, vol. 20, no. 2, pp. 365–373, 2004.
[14] S. Stramigioli, C. Secchi, A. van der Schaft, and C. Fantuzzi., "A novel theory for sample data system passivity," in *Proceedings of the IEEE/RSJ International Conference on Intelligent Robots and Systems*, Lausanne, Switzerland, 2002, pp. 1936–1941.
[15] J. Artigas, C. Preusche, G. Hirzinger, G. Borghesan, and C. Melchiorri, "Bilateral energy transfer in delayed teleoperation on the time domain," in *IEEE International Conference on Robotics and Automation*, 2008, pp. 671–676.
[16] M. Tavakoli, A. Aziminejad, R. Patel, and M. Moallem, "High-fidelity bilateral teleoperation systems and the effect of multimodal haptics," *IEEE Transactions on Systems, Man and Cybernetics – Part B*, vol. 37, no. 6, pp. 1512–1528, December 2007.
[17] K. Ogata, *Discrete-Time Control Systems*, 2nd ed. Prentice Hall, 1995.
[18] M. Fadali and A. Visioli, *Digital control engineering: analysis and design*, ser. Electronics & Electrical. Academic/Elsevier, 2009.
[19] A. Oppenheim, A. Willsky, and I. Young, *Signals and systems*, ser. Prentice-Hall signal processing series. Prentice-Hall International, 1996.
[20] K. Kosuge, T. Itoh, and T. Fukuda, "Scaled telemanipulation with communication time delay," in *Robotics and Automation, 1996. Proceedings., 1996 IEEE International Conference on*, vol. 3, 1996, pp. 2019 –2024 vol.3.
[21] H. C. Cho and J. H. Park, "Impedance controller design of Internet-based teleoperation using absolute stability concept," in *IEEE/RSJ International Conference on Intelligent Robots and Systems, 2002*, vol. 3, 2002, pp. 2256 – 2261 vol.3.

APPENDIX

Lemma 1: For any arbitrary function $V(j\omega)$ and $\bar{C}(\omega)$

$$\int_{-\infty}^{\infty} \bar{C}(\omega) \sum_{n=-\infty}^{\infty} \frac{V(j\omega + jn\omega_s)}{j\omega + jn\omega_s} \left[\frac{V(j\omega)}{j\omega}\right]^c d\omega \tag{36}$$

The integral (36) does not change if $\bar{C}(\omega)$ is replaced with its real part $\mathrm{Re}\{\bar{C}(\omega)\}$.

Lemma 2: For any arbitrary function $V(j\omega)$ and positive definite $\bar{C}^+(\omega)$

$$\int_{-\infty}^{\infty} \bar{C}^+(\omega) \sum_{n=-\infty}^{\infty} \frac{V(j\omega + jn\omega)}{j\omega + jn\omega} \left[\frac{V(j\omega)}{j\omega}\right]^c d\omega > 0 \tag{37}$$

Lemma 3: For $V(j\omega)$ as in (12) and any arbitrary negative definite $\bar{C}^-(\omega)$ we have

$$\int_{-\infty}^{\infty} \bar{C}^-(\omega) \sum_{n=-\infty}^{\infty} \frac{V(j\omega + jn\omega)}{j\omega + jn\omega} \left[\frac{V(j\omega)}{j\omega}\right]^c d\omega >$$
$$\int_{-\infty}^{\infty} \bar{C}^-(\omega) \sum_{n=-\infty}^{\infty} \frac{1}{(\omega + n\omega_s)^2} V(j\omega)V^c(j\omega)d\omega \tag{38}$$

Lemma 4: For any arbitrary complex numbers of X and Y, $-XY^c - X^cY \leq XX^c + YY^c$, where superscript ^{c} stands for complex conjugate.

Lemma 5: A sufficient condition for satisfying the passivity condition

$$\int_{-\infty}^{\infty} \bar{C}^-(\omega) \sum_{n=-\infty}^{\infty} \frac{1}{(\omega + n\omega_s)^2} V(j\omega)V^c(j\omega)d\omega +$$
$$\int_{-\infty}^{\infty} b_m V_m(j\omega)V_m^c(j\omega)d\omega + \int_{-\infty}^{\infty} b_s V_s(j\omega)V_s^c(j\omega)d\omega > 0 \tag{39}$$

is

$$b_m > \frac{T}{1-\cos\omega T} \mathrm{Re}\left\{(1-e^{-j\omega T})C_m(e^{j\omega T})\right\}$$
$$b_s > \frac{T}{1-\cos\omega T} \mathrm{Re}\left\{(1-e^{-j\omega T})C_s(e^{j\omega T})\right\} \tag{40}$$